

# ARTalk: Speech-Driven 3D Head Animation via Autoregressive Model

Xuangeng Chu<sup>1</sup> Nabarun Goswami<sup>1</sup> Ziteng Cui<sup>1</sup> Hanqin Wang<sup>1</sup> Tatsuya Harada<sup>1,2</sup>

## Abstract

Speech-driven 3D facial animation aims to generate realistic lip movements and facial expressions for 3D head models from arbitrary audio clips. Although existing diffusion-based methods are capable of producing natural motions, their slow generation speed limits their application potential. In this paper, we introduce a novel autoregressive model that achieves real-time generation of highly synchronized lip movements and realistic head poses and eye blinks by learning a mapping from speech to a multi-scale motion codebook. Furthermore, our model can adapt to unseen speaking styles using sample motion sequences, enabling the creation of 3D talking avatars with unique personal styles beyond the identities seen during training. Extensive evaluations and user studies demonstrate that our method outperforms existing approaches in lip synchronization accuracy and perceived quality. Demos and codes are available at [https://xg-chu.site/project\\_artalk/](https://xg-chu.site/project_artalk/).

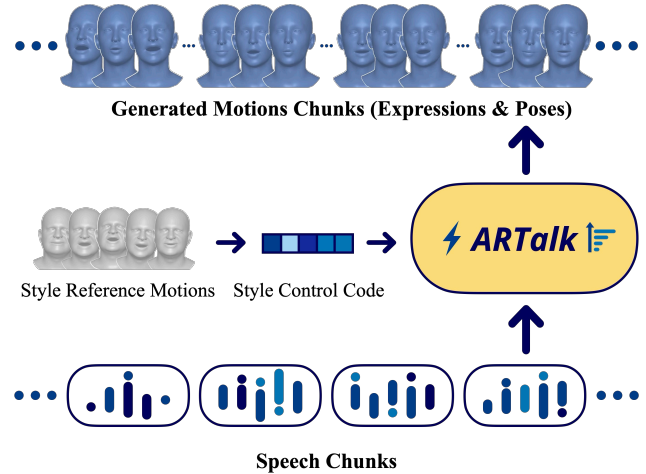


Figure 1. We present ARTalk, a framework for speech-driven 3D facial motion generation. Our method learns a mapping from speech to a multi-scale motion codebook, enabling the real-time generation of realistic and diverse animation sequences.

## 1. Introduction

Speech-driven 3D facial animation has attracted significant attention in both academia and industry due to its broad applications in virtual reality, game animation, film production, and human-computer interaction. This task focuses on generating natural and synchronized facial expressions, particularly lip movements, along with realistic head motions directly from speech input. In recent years, many exploratory methods have significantly enhanced the performance of speech-driven motion generation tasks. However, generating natural and human-like motions remains challenging due to the inherently complex many-to-many mapping between speech and facial or head movements. Capturing these intricate relationships is crucial for creating realistic animations.

Some existing methods, such as (Richard et al., 2021; Xing

<sup>1</sup>The University of Tokyo, Tokyo, Japan <sup>2</sup>RIKEN AIP, Tokyo, Japan. Correspondence to: {xuangeng.chu, nabarungoswami, cui, wang, harada}@mi.t.u-tokyo.ac.jp.

et al., 2023; Sung-Bin et al., 2024; Nocentini et al., 2024), employ autoregressive models to predict deformation offsets on meshes for speech-driven motion generation. However, due to the high complexity of meshes in 3D space, these approaches often fail to fully capture the many-to-many relationships between speech and motion. This limitation frequently results in overly smooth non-lip facial expressions that lack realism. Recent works leveraging diffusion models (Ho et al., 2020; Tevet et al., 2023; Stan et al., 2023; Sun et al., 2024) have demonstrated impressive results in generative tasks, including speech-driven motion. For instance, FaceDiffuser (Stan et al., 2023) employs diffusion to generate motions directly on meshes, while DiffPoseTalk (Sun et al., 2024) generates facial expressions and head motions using diffusion on FLAME (Li et al., 2017) blendshapes, achieving natural results. However, these methods involve computationally expensive diffusion processes and cannot perform real-time and low-latency motion generation. Meanwhile, multi-scale autoregressive models (Tian et al., 2024) have shown success in image autoregressive generation tasks, offering fast and high-quality results. However, these models are designed for single multi-scale samples

instead of temporal motions, and thus cannot be directly applied to speech-to-motion generation tasks.

To address the challenges of achieving high-quality, natural, and fast speech-driven motion generation while overcoming these limitations, we propose a novel method based on sliding temporal windows and multi-scale autoregression. Our method divides speech into time windows for generation, which is important for low-latency action generation. We extend the VQ autoencoder to encode multi-scale motion codes across two consecutive time windows, enabling effective handling of temporal sequence data. Additionally, we design a novel autoregressive generator that conditionally generates multi-scale motion codes based on the speech input of the current time window and previously generated motions. This design allows our autoregressive model to perform high-quality multi-scale generation within each time window while maintaining temporal continuity across windows. Furthermore, we integrated a transformer-based style encoder to extract style codes from sample motion segments, enabling our model to generate stylized motions that reflect unique individual characteristics while reducing the complexity of the many-to-many mapping between speech and motion. These innovations enable our method to achieve personalized and high-fidelity lip motions, facial expressions and head motion generation, making it suitable for a wide range of speech-driven downstream tasks.

Our main contributions are as follows:

- We propose ARTalk, a novel autoregressive framework capable of generating natural 3D facial motions with head poses in real time.
- We design a novel encoder-decoder that encode motions from consecutive time windows to produce temporally dependent multi-scale motion representations.
- We introduce a novel conditional autoregressive generator on temporal and feature scales, enabling motion generations tightly aligned with speech conditions and consistent across time windows.

## 2. Related Work

### 2.1. Speech-Driven 3D Facial Animation

Research on audio-driven 3D motion generation has been an area of interest for decades, with methods evolving significantly over time. Early approaches (Taylor et al., 2012; Xu et al., 2013; Edwards et al., 2016) relied primarily on procedural methods, which segmented speech into phonemes and mapped them to predefined visemes through handcrafted rules. Although procedural methods provide explicit control over the generated animations, they typically require complex parameter tuning and fail to capture the diversity and complexity of real-world speaking styles. As a result,

Table 1. Comparison across methods, including style adaptation during inference (w/ Style), head pose generation (w/ Pose), and real-time capability (Real-time). ARTalk (ours) is the only method to achieve all three features, demonstrating its comprehensive advantages over baseline methods.

METHOD	W/ STYLE	W/ POSE	REAL-TIME
FACEFORMER (FAN ET AL., 2022)	✗	✗	✗
CODETALKER (XING ET AL., 2023)	✗	✗	✗
SELFTALK (PENG ET AL., 2023A)	✗	✗	✓
FACEDIFFUSER (STAN ET AL., 2023)	✗	✗	✗
MULTITALK (SUNG-BIN ET AL., 2024)	✓	✗	✗
SCANTALK (NOCENTINI ET AL., 2024)	✗	✗	✗
DIFFPOSETALK (SUN ET AL., 2024)	✓	✓	✗
ARTALK (OURS)	✓	✓	✓

procedural methods struggled to deliver animations that appeared both natural and adaptable to varying speech dynamics. In recent years, learning-based approaches (Fan et al., 2022; Xing et al., 2023; Sun et al., 2024; Daněček et al., 2023; Peng et al., 2023b; Yang et al., 2024) have advanced rapidly, addressing these limitations and enabling more natural and expressive facial animations. Additionally, some approaches (Yi et al., 2022; Ye et al., 2024; Zhang et al., 2023; Tan et al., 2024) focus on directly generating talking head videos without explicitly modeling motion. However, this limits their ability to integrate with motion-driven downstream applications, restricting their broader applicability.

### 2.2. Autoregressive 3D Facial Motion Generation

Autoregressive (AR) methods model the temporal sequence of facial motion in a step-by-step manner. These methods typically leverage pre-trained speech model features (Baeviski et al., 2020; Hsu et al., 2021; Défossez et al., 2024) as speech representations, which are subsequently mapped to 3D deformable model parameters or 3D meshes via neural networks. For example, FaceFormer (Fan et al., 2022) autoregressively predicts the continuous facial motion parameters while MeshTalk (Richard et al., 2021) learns a prior over categorical expression tokens. CodeTalker (Xing et al., 2023) and MultiTalk (Sung-Bin et al., 2024) tokenize facial motions with a VQ-VAE and train a transformer decoder to predict subsequent motion tokens based on audio features. Learn2Talk (Zhuang et al., 2024) augments FaceFormer with lip-sync and lip-reading losses, improving alignment with speech. MMHead (Wu et al., 2024) provides text descriptions as an extra condition for controlling the generated motion. However, these methods also show limitations. Temporal autoregressive modeling often under represents motion within each time window, leading to overly smooth lip movements and failing to capture the complex speech-to-motion mapping. This issue becomes more pronounced with larger and more diverse datasets. Additionally, many

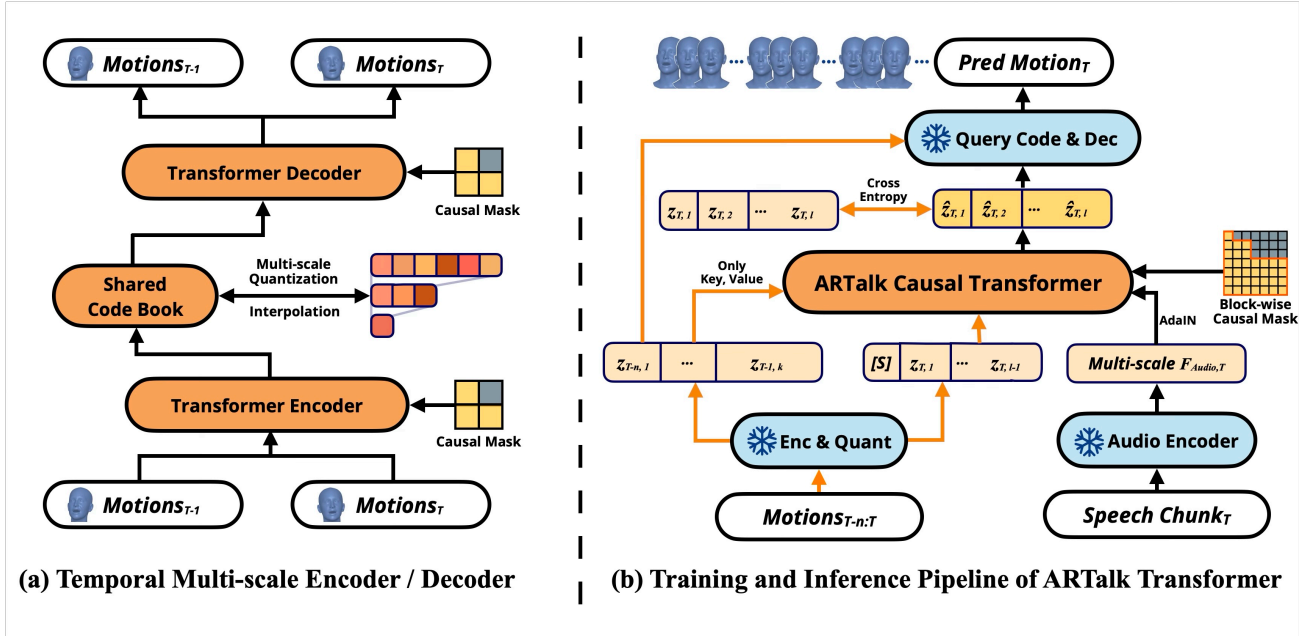


Figure 2. ARTalk involves two separated parts. (a) shows our temporal multi-scale VQ autoencoder. It encodes motion sequences into multi-scale token maps  $[M_{k_1}, M_{k_2}, \dots, M_{K}]$  using a shared codebook and causal masking on temporal. (b) shows The ARTalk Causal Transformer, where training uses ground truth tokens with a block-wise causal attention mask, and inference autoregressively predicts motion tokens conditioned on speech features and last scale tokens and last time window motions.

approaches (Fan et al., 2022; Xing et al., 2023; Sung-Bin et al., 2024) rely on a predefined set of style labels to reduce the complexity of the mapping, which limits their ability to adapt to new individuals and styles.

### 2.3. Diffusion based 3D Facial Motion Generation

Diffusion models (Ho et al., 2020; Zhu et al., 2023; Alexanderson et al., 2023; Stan et al., 2023; Ma et al., 2024; Sun et al., 2024) have recently gained traction for generative tasks because of their strong modeling capacities. FaceDiffuser (Stan et al., 2023) conditions a diffusion model on audio features to predict displacements from a neutral template. More recently, FaceTalk (Aneja et al., 2024) employs a diffusion model on expression coefficients with cross-attention to wav2vec2 (Baeovski et al., 2020) features, while DiffSpeaker (Ma et al., 2024) utilizes biased conditional attention for a diffusion-driven synthesis pipeline. Scantalk (Nocentini et al., 2024) uses a DiffusionNet (Sharp et al., 2022) structure to overcome the fixed topology limitation and perform diffusion on arbitrary meshes. Similarly, DiffPoseTalk (Sun et al., 2024) uses a diffusion-based transformer decoder to generate both expression and pose (blendshapes) conditioned on audio and learned style features. Going beyond motion, LetsTalk (Zhang et al., 2024) adopts a spatiotemporal diffusion approach to synthesize entire video frames.

Although these methods generate high-fidelity and realistic facial motion, their iterative sampling steps can be computationally expensive and may limit real-time applicability.

In this paper, we leverage FLAME (Li et al., 2017) as our motion representation and propose a novel autoregressive framework for speech-driven motion generation. It not only outperform current diffusion models in generating facial motion, but it also achieves real-time speed and produce natural head poses. A comparison of our method with existing approaches is shown in Table 1. Our method enables arbitrary style inference, allowing stylized motion generation at inference time by providing an example motion clip. Additionally, our method generates both facial expressions and head poses while maintaining real-time performance.

## 3. Method

We provide an overview of our method in Figure 2. We adopt the widely used 3DMM (Li et al., 2017) as the facial representation and leverage a multi-scale VQ autoencoder model to train and obtain a multi-scale motion codebook along with its corresponding encoder-decoder, enabling a discrete representation of the motion space. Subsequently, we train a multi-scale autoregressive model to map speech information to the discrete motion space.

In the following subsections, Section 3.1 details the problem definition and the 3DMM representation, Section 3.2 explains the multi-scale motion VQ autoencoder model, Section 3.3 introduces the multi-scale autoregressive model.

### 3.1. Preliminaries

We adopt the widely used 3D morphable model (3DMM) FLAME (Li et al., 2017) to represent facial motion, where each frame is parameterized by shape  $\beta$ , expression  $\psi$ , and pose  $\theta$ . Given these parameters, the 3D face mesh, consisting of 5,023 vertices, is reconstructed through blend shape and rotation operations. Compared to previous methods (Fan et al., 2022; Xing et al., 2023; Peng et al., 2023a; Nocentini et al., 2024) that directly model the mesh, FLAME simplifies motion modeling by converting complex vertex movements into lower-dimensional blend shape parameters while preserving expression and motion details.

We define the motion vector  $\mathbf{M} \in \mathbb{R}^{K \times D}$  as the concatenation of per-frame expression and pose parameters over  $K$  frames, i.e.,  $\mathbf{M} = [\psi \ \theta]$ . The corresponding vertex coordinates  $\mathbf{V} \in \mathbb{R}^{K \times N \times 3}$  store the 3D positions of  $N$  mesh vertices per frame, where  $\mathbf{V}_{\text{lips}} \subset \mathbf{V}$  denotes the subset corresponding to the lip region, which is particularly important for speech related expression modeling. Further details on 3DMM can be found in the supplementary material.

### 3.2. Temporal Multi-scale VQ Autoencoder

Predicting motion frames from speech is a discrete task involving highly dense temporal sequences and complex mappings. Inspired by the success of discrete representations in image and motion generation (Xing et al., 2023; van den Oord et al., 2017; Zhou et al., 2022) and the effectiveness of multi-scale encoding in (Tian et al., 2024), we propose a temporal multi-scale VQ autoencoder to efficiently model motion dynamics.

The input motion sequence, consisting of  $K$  frames, is first processed by a Transformer encoder, which extracts temporal features and maps them into a latent space. These representations are then quantized using a multi-scale codebook that captures motion information at varying temporal resolutions  $[k_1, k_2, \dots, K]$ , producing discrete tokens. The Transformer decoder reconstructs the motion from these discrete embeddings, attending to both local and long-range dependencies.

**Multi-scale residual VQ.** To progressively refine motion representations, we adopt a residual vector quantization approach:

$$\begin{aligned} \mathbf{h}^{(l)} &= \text{Interp}(\text{Quant}(\mathbf{r}^{(l-1)}), k_l), \\ \mathbf{r}^{(l)} &= \mathbf{r}^{(l-1)} - \mathbf{h}^{(l)}, \end{aligned} \quad (1)$$

for  $l = 1, \dots, L$ , where  $\mathbf{r}^{(0)}$  is the encoder output. The

function  $\text{Quant}(\cdot)$  assigns features to the closest codebook entries, while  $\text{Interp}(\cdot, k_l)$  adjusts resolutions to ensure smooth transitions. By accumulating the outputs  $\mathbf{h}^{(l)}$  across scales, the model retains high fidelity while removing redundancy in a structured manner.

Residual accumulation at the finest scale  $K$  mitigates information loss, while downsampling via region-based interpolation enhances efficiency. We use a *shared* codebook across scales to maintain a unified motion space and simplify autoregressive modeling. This strategy improves temporal consistency and preserves stylistic coherence across different resolutions.

**Temporal causal reasoning.** To ensure stability over extended sequences, we incorporate a causal reasoning mechanism that enforces cross-window consistency. Instead of generating frames independently, our approach considers two consecutive time windows,  $T - 1$  and  $T$ . During training and inference, causal masks are applied, ensuring that predictions for  $T$  depend only on previously observed information from  $T - 1$ , without leaking future details. This prevents temporal discontinuities and enhances the smoothness of long-term motion.

By integrating multi-scale residual quantization with causal reasoning and Transformer-based encoding/decoding, our method ensures both fine-grained expressiveness and long-term coherence in generated motion sequences.

#### Training objectives.

To train the VQ autoencoder, we use a hybrid loss function balancing motion accuracy, temporal smoothness, and codebook stability.

The reconstruction loss enforces alignment between predicted motion vectors  $M'$  and the ground truth  $M$ , with additional constraints on lip and facial vertices:

$$L_{\text{recon}} = \|\hat{M} - M\|_1 + w_{\text{lips}} \|\hat{V}_{\text{lips}} - V_{\text{lips}}\|^2 + \|\hat{V} - V\|^2 \quad (2)$$

To ensure smooth transitions, we penalize velocity and acceleration differences:

$$L_{\text{vel}} = \|(\hat{V}_{1:} - \hat{V}_{:-1}) - (V_{1:} - V_{:-1})\|^2, \quad (3)$$

$$L_{\text{smooth}} = \|\hat{V}_{2:} - 2\hat{V}_{1:-1} + \hat{V}_{:-2}\|^2. \quad (4)$$

We also apply the standard VQ losses which we term as  $L_{\text{cb}}$  to encourage stable VQ assignments and prevent mode collapse.

The final training objective is:

$$L_{\text{VQ}} = L_{\text{recon}} + \lambda_{\text{vel}} L_{\text{vel}} + \lambda_{\text{smooth}} L_{\text{smooth}} + L_{\text{cb}}, \quad (5)$$

where  $\lambda_{\text{vel}}$  and  $\lambda_{\text{smooth}}$  control the temporal constraints.

By jointly optimizing these terms, the model learns compact yet expressive motion representations, ensuring high-fidelity synthesis with strong temporal coherence.

### 3.3. Speech-to-Motion Autoregressive Model

After training the VQ autoencoder (Section 3.2), we obtain discrete codes  $\{\mathbf{z}_T^{(l)}\}$  at multiple resolutions  $k_l$  for each time window  $T$ , where  $l = 1, \dots, L$  spans from coarsest ( $k_1$ ) to finest ( $k_L$ ). To ensure long-term temporal coherence, we model these codes with a Transformer that is autoregressive *across scales* ( $1 \rightarrow L$ ) and *across adjacent windows* ( $T - 1 \rightarrow T$ ).

**Architecture.** Figure 2(b) illustrates the AR model, where orange arrows mark training-only components. A pre-trained HuBERT (Hsu et al., 2021) encoder extracts speech features  $\mathbf{a}_T$ , resampled to each scale  $k_l$ . A style token  $\mathbf{s}$  encodes speaker identity (Sun et al., 2024). Given the previous window’s finest-scale codes  $\mathbf{z}_{T-1}^{(L)}$ , we predict  $\mathbf{z}_T^{(1)}, \dots, \mathbf{z}_T^{(L)}$  for the current window.

**Two-level autoregression.** Within each window  $T$ , the codes are generated scale by scale:

$$p(\{\mathbf{z}_T^{(l)}\}_{l=1}^L | \mathbf{z}_{T-1}^{(L)}, \mathbf{a}_T, \mathbf{s}) = \prod_{l=1}^L p(\mathbf{z}_T^{(l)} | \mathbf{z}_T^{(<l)}, \mathbf{z}_{T-1}^{(L)}, \mathbf{a}_T, \mathbf{s}), \quad (6)$$

where  $\mathbf{z}_T^{(<l)}$  denotes codes at all coarser scales. Inside each scale  $l$ , tokens are predicted *in parallel* (blockwise) while attending causally to previously generated scales and the previous window.

**Training and inference.** During training, ground-truth codes  $\{\mathbf{z}_T^{(l)\text{(gt)}}\}$  supervise the model via cross-entropy:

$$L_{\text{AR}} = - \sum_T \sum_{l=1}^L \log p(\mathbf{z}_T^{(l)\text{(gt)}} | \mathbf{z}_T^{(<l)\text{(gt)}}, \mathbf{z}_{T-1}^{(L)\text{(gt)}}, \mathbf{a}_T, \mathbf{s}). \quad (7)$$

At inference, we sample or select each scale’s codes in sequence, conditioned on  $\mathbf{z}_{T-1}^{(L)}$ ,  $\mathbf{a}_T$ , and  $\mathbf{s}$ . Repeating this process over windows yields motion sequences that remain temporally coherent and stylistically consistent throughout.

## 4. Experiments

**Datasets.** We use the TFHP dataset proposed by Sun et al. (2024) to train our model, which consists of 1,052 video clips from 588 subjects, with a total duration of approximately 26.5 hours. All videos are tracked at 25 fps, resulting in approximately 2,385,000 action frames. For training and evaluation, we adopt the train/test split provided in the original paper (Sun et al., 2024). Furthermore, we evaluate the generalization performance of our model on the test split of

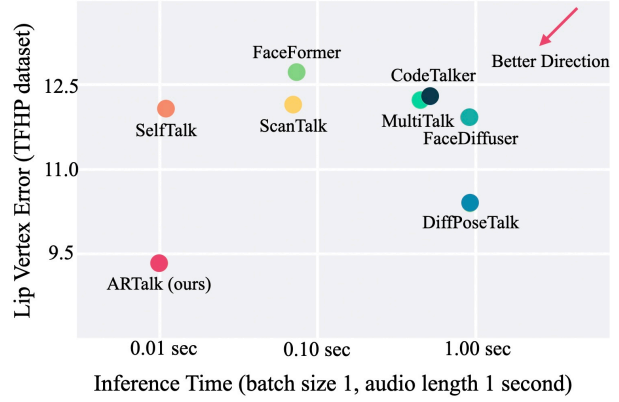


Figure 3. Comparison of runtime efficiency and performance across different methods.

the widely used VOCASET dataset (Cudeiro et al., 2019). The test split consists of 80 audiovisual sequence pairs from 2 subjects. To adapt VOCASET to our method, we track the FLAME parameters at 25 fps and conduct evaluation on our tracked data. It is worth noting that we don’t use the VOCASET training split to train or fine-tune our method.

**Implementation Details.** Our method is implemented on the PyTorch framework (Paszke et al., 2017). In the first stage, we train our VQ autoencoder to obtain a multi-scale motion codebook. The size of the motion codebook is 256 and the code dimension is 64. The motion codebook consists of 256 entries, each with a code dimension of 64. The time window size is 100 frames (4 seconds), and the multi-scale levels are [1, 5, 25, 50, 100]. During this stage, we used the AdamW optimizer with a learning rate of  $1.0e-4$ , a total batch size of 64, and trained for 50,000 iterations. In the second stage, we train the multi-scale autoregressive model using the AdamW optimizer with the same learning rate of  $1.0e-4$  and a batch size of 64 for 50,000 iterations. During this stage, we employ a frozen pre-trained HuBERT (Hsu et al., 2021) backbone without fine-tuning.

All training was conducted on one NVIDIA Tesla A100 GPU, requiring a total of approximately 13 GPU hours (5 hours for the first stage and 8 hours for the second stage), demonstrating efficient training resource utilization. During inference, our method needs only 0.01 seconds to generate motions for 1 second on an NVIDIA Tesla A100 GPU and 0.057 seconds on an Apple M2 Pro chip, showcasing high inference efficiency and low latency. For more implementation details, please refer to the supplementary materials.

### 4.1. Quantitative Results

Based on previous studies (Richard et al., 2021; Fan et al., 2022; Xing et al., 2023; Nocentini et al., 2024; Sun et al., 2024), we adopted two quantitative metrics, the lip vertex er-

Table 2. Quantitative results on the TFHP (Sun et al., 2024) dataset. We use colors to denote the first and second places respectively. \* indicates that the method was not trained on TFHP, while all other methods were trained or fine-tuned on TFHP.

METHOD	LVE ↓	FFD ↓	MOD ↓
FACEFORMER (FAN ET AL., 2022)	12.72	22.06	2.73
CODETALKER (XING ET AL., 2023)	12.28	22.38	2.60
SELFTALK (PENG ET AL., 2023A)	12.07	23.74	2.57
FACEDIFFUSER (STAN ET AL., 2023)	11.92	22.17	2.55
MULTITALK* (SUNG-BIN ET AL., 2024)	12.23	24.42	2.48
SCANTALK* (NOCENTINI ET AL., 2024)	12.14	21.02	3.20
DIFFPOSETALK (SUN ET AL., 2024)	10.39	20.15	2.07
ARTALK (OURS)	9.34	18.15	1.81

Table 3. Quantitative results on the VOCASET-Test (Cudeiro et al., 2019) dataset. We use colors to denote the first and second places respectively. \* indicates that the method was not trained on VOCASET. It is worth noting that our method is **not** trained or fine-tuned on VOCASET.

METHOD	LVE ↓	FFD ↓	MOD ↓
FACEFORMER (FAN ET AL., 2022)	8.28	15.62	1.89
CODETALKER (XING ET AL., 2023)	7.73	18.86	1.81
SELFTALK (PENG ET AL., 2023A)	7.71	28.70	1.79
FACEDIFFUSER (STAN ET AL., 2023)	8.00	21.46	1.84
MULTITALK* (SUNG-BIN ET AL., 2024)	12.33	25.11	2.82
SCANTALK (NOCENTINI ET AL., 2024)	7.15	15.56	1.61
DIFFPOSETALK* (SUN ET AL., 2024)	10.01	20.64	2.29
ARTALK (OURS)*	7.57	15.49	1.78

ror (LVE) (Richard et al., 2021) and the upper face dynamic deviation (FDD) (Xing et al., 2023), to evaluate the generated facial motions. LVE calculates the maximum L2 error of all lip vertices for each frame, evaluating the largest deviation between predicted and ground truth lip positions. FDD calculates the standard deviation of the motion of each upper facial vertex over time between predictions and ground truth, evaluating the consistency of upper facial motion, which is closely related to speaking styles. Additionally, we use a similar metric as Sun et al. (2024), mouth opening distance (MOD), to more accurately assess the stylistic similarity of mouth opening movements. MOD measures the average difference in mouth opening region between predictions and ground truth. Compared to LVE, MMD focuses more on the similarity of mouth opening styles and is less sensitive to temporal lip synchronization. For the partitioning of the lip area and upper face, we used the mask partitioning officially provided by FLAME (Li et al., 2017). The lip region contains 254 points, while the upper face, including the eye region and forehead, contains 884 points.

We present the quantitative comparison on TFHP dataset (Sun et al., 2024) in Table 2. The baseline methods Face-

Former (Fan et al., 2022), CodeTalker (Xing et al., 2023), SelfTalk (Peng et al., 2023a), and FaceDiffuser (Stan et al., 2023) are all mesh-based approaches and cannot directly generalize to arbitrary styles or new meshes. To ensure a fair comparison, we retrained these methods on meshes generated from the TFHP dataset. For MultiTalk (Sung-Bin et al., 2024), which is trained on FLAME meshes and supports language-based stylization, we directly used its English style for evaluation. ScanTalk claims to work on arbitrary meshes, so we use the officially provided pre-trained weights. For DiffPoseTalk, we directly used its pre-trained weights on the TFHP dataset (including head pose) for evaluation. The results in the Table 2 show that our method achieving significant improvements in lip synchronization accuracy (LVE) and style alignment (FFD and MOD), indicating that our method not only achieves precise lip synchronization but also effectively captures personalized speaking styles.

To demonstrate the generalizability of our method, we evaluated it on the VOCASET dataset (Cudeiro et al., 2019). The results are presented in Table 3. Notably, for some baseline methods (Fan et al., 2022; Xing et al., 2023; Peng et al., 2023a; Stan et al., 2023; Nocentini et al., 2024), we used their pre-trained weights on VOCASET, whereas our method was **not** trained or fine-tuned on this dataset. Despite this, our method achieved highly competitive performance and outperformed most baseline methods specifically trained on this dataset. For MultiTalk (Sung-Bin et al., 2024) and DiffPoseTalk (Sun et al., 2024) which designed with style generalization capabilities, we followed the same strategy as with our method by directly testing it on the VOCASET dataset without any additional training or fine-tuning. The results indicate that our method surpasses them in terms of generalization ability, further verifying the robustness of our method in handling unseen styles and data.

We also present a comparison of LVE and efficiency in Figure 3. Although our model adopts a two-level autoregressive framework, it remains more efficient than fully autoregressive methods. This efficiency is achieved by utilizing longer window lengths while retaining only the past 4 seconds of motion frames. Additionally, frames within each scale are generated in parallel within the window, further improving computational efficiency.

## 4.2. Qualitative Results

In Figure 4, we present a qualitative comparison between our method and other baseline approaches. Our method demonstrates excellent lip synchronization, accurately capturing various phonetic elements. Furthermore, the generated results exhibit realistic facial expressions and mouth opening, closely matching the style of the ground truth. Notably, our method also generates realistic blinking and head movements, which are implicitly learned and encoded within the

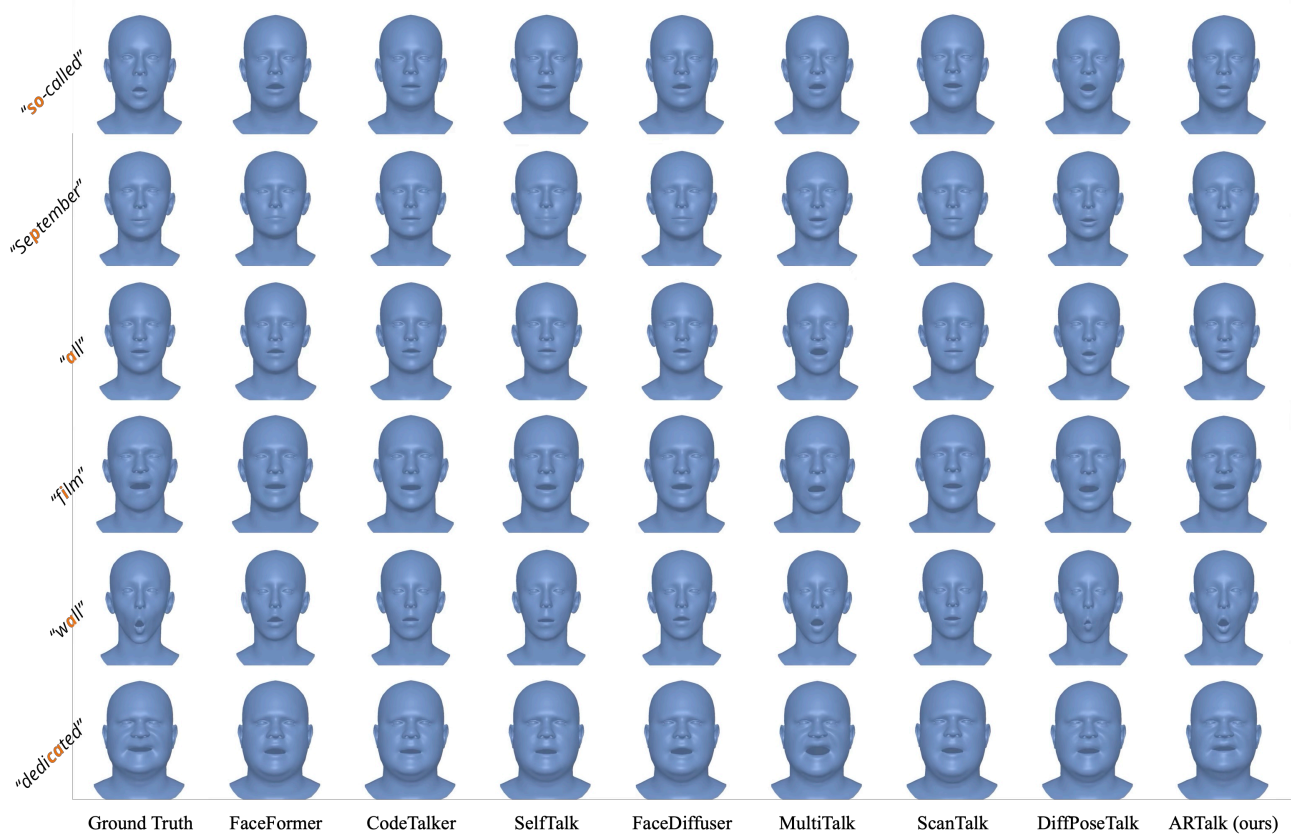


Figure 4. Qualitative comparison with existing methods (all head poses fixed). The first four rows are from the TFHP dataset, and the last two rows are from the VOCASET dataset. Our method shows better alignment with the ground truth in expression style, mouth dynamics, and lip synchronization. Additional results are available in the supplementary materials and demo videos.

Table 4. User study results.

METHOD	SYNC (%)	NAT-EXP (%)	STYLE (%)	NAT-POSE (%)
VS. FACEFORMER	75.0	89.3	88.1	-
VS. CODETALKER	84.5	86.9	92.9	-
VS. SELFTALK	85.7	89.3	91.7	-
VS. FACEDIFFUSER	88.1	90.4	86.9	-
VS. MULTITALK	78.6	76.2	78.6	-
VS. SCANTALK	88.1	90.5	90.5	-
VS. DIFFPOSETALK	63.1	59.5	60.7	58.3

motion codebook. Additional qualitative evaluation results are available in the supplementary videos.

### 4.3. User Study

User studies are a reliable approach for evaluating 3D talking heads. To comprehensively compare our method with baseline methods (Fan et al., 2022; Xing et al., 2023; Peng et al., 2023a; Stan et al., 2023; Sung-Bin et al., 2024; Nocentini et al., 2024; Sun et al., 2024), we conducted a user study focusing on four key metrics: lip synchronization,

facial expression naturalness, style consistency and head pose naturalness.

Given that head movements can significantly influence users’ evaluation of lip synchronization, the study was divided into two parts. In the first part, videos with fixed head poses were rendered across all methods to assess lip synchronization and facial expression realism and style consistency. In the second part, videos with dynamic head poses were rendered to evaluate style consistency and head pose naturalness. All comparisons were conducted using pairwise comparisons, where motions generated by our method and a competing baseline were displayed side by side, along with the ground truth provided as a reference for users. After watching the videos, users selected the animation they perceived as better based on their subjective preference. The proportion of user selections was calculated to quantify satisfaction.

As presented in Table 4, our method significantly outperformed the baseline methods in lip synchronization, style consistency and facial expression realism. Furthermore, our method achieved superior head pose naturalness com-

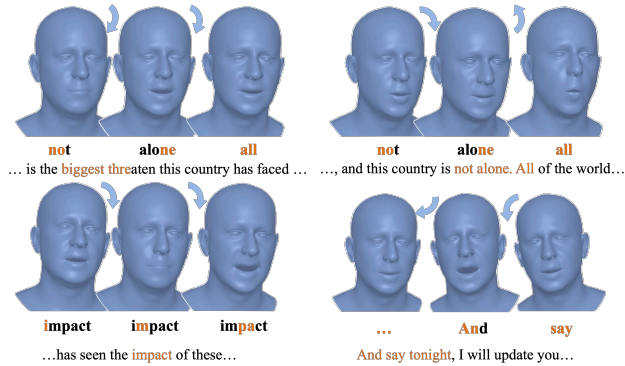


Figure 5. Qualitative results of head pose. When certain words are stressed or when accents occur, the model produces nodding motions similar to human behavior. Additionally, during transitions between different speech styles or sentence breaks, the head naturally turns, reflecting realistic conversational dynamics.

pared to DiffPoseTalk (Sun et al., 2024), demonstrating its comprehensive advantages.

#### 4.4. Ablation study

**Multi-Scale Autoregression.** To validate the importance of multi-scale autoregressive modeling within a single time window, we conducted experiments by removing the multi-scale autoregressive mechanism entirely. The results shown in Table 5 indicate a significant drop in generation accuracy without multi-scale autoregression. We attribute this decline to the model’s inability to fully capture the complex details of the speech-to-motion mapping without the hierarchical structure provided by multi-scale modeling.

**Temporal Encoder and Temporal Autoregression.** To assess the necessity of temporal encoding and autoregression across time windows, we replaced our proposed temporal encoder and autoregressive model with a standard multi-scale encoder and a single-window multi-scale autoregressive model, respectively. As shown in Table 5, the absence of temporal modeling in VQ autoencoder or autoregressive both result in degraded generation quality. Additionally, we also observed temporal discontinuities in the motion sequences, further emphasizing the critical role of our temporal design in achieving smooth and coherent outputs.

**Speaker Style Embedding.** We also evaluated the effect of removing the speaker style feature, which serves as the starting condition for the autoregressive process. Without this feature, the complexity of the many-to-many mapping between speech and motion increases significantly, and the generated motions lack personalized style. As reflected in Table 5, the removal of style features causes a substantial decline in generation quality, highlighting their importance in achieving stylistic and expressive outputs.

**Key Hyperparameter Choices.** We explored different num-

Table 5. Ablation results on TFHP dataset.

METHOD	LVE↓	FFD↓	MOD ↓
W/O MULTI-SCALE AR	14.14	22.04	3.06
W/O TEMPORAL VQ	9.82	18.60	1.86
W/O TEMPORAL AR	9.97	18.71	1.99
W/O STYLE EMBEDDING	11.80	21.46	2.37
MOTION CLIP LENGTH 8	11.73	24.89	2.25
MOTION CLIP LENGTH 25	10.20	19.00	1.97
MOTION CLIP LENGTH 50	9.78	<b>18.03</b>	1.89
ARTALK (FULL)	<b>9.34</b>	18.15	<b>1.81</b>

ber of motion frames within a single time window, which is critical for our method. Specifically, we tested window lengths of 8, 25, 50 frames. For a window length of 8, we used a multi-scale sequence of [1,2,4,8], while for 25 and 50, we adopted [1,5,10,15,25] and [1,5,10,25,50], respectively. The results, presented in Table 5, demonstrate that the choice of window size significantly impacts performance. However, the window size depends heavily on the downstream task characteristics, such as whether the input consists of streaming audio chunks. In general, longer temporal windows generally produce better results. In this paper, we chose a window length of 100 frames and a multi-scale sequence of [1, 5, 25, 50, 100] as it is consistent with previous work such as DiffPoseTalk (Sun et al., 2024) and achieves a good balance between quality and efficiency.

## 5. Discussion and Conclusion

In this paper, we introduced ARTalk, a novel framework for generating 3D facial and head motions from speech. The core innovation of our method lies in the temporal multi-scale autoencoder and the ARTalk autoregressive Transformer, which together ensure temporal consistency and precise motion generation. Our experimental results demonstrate that ARTalk outperforms state-of-the-art baselines in terms of lip synchronization, expression naturalness and style consistency, while maintaining real-time generation capabilities. We believe that the strong generalization ability of ARTalk make it a promising solution for a wide range of applications, including virtual avatars, language training, and animation production for gaming and movies.

**Limitations and future work.** While ARTalk demonstrates strong performance in lip synchronization and expressions, a current limitation is that head motions are primarily driven by speech prosody (rhythm and emphasis) rather than semantic context. Addressing the cultural and semantic nuances of head gestures, such as nodding or shaking to indicate affirmation, would require broader and more diverse datasets and fine-grained head pose control, which we leave as future work. We hope that our work lays a solid foundation for the further research of 3D talking head generation.



## Impact Statement

Given that our method can generate highly realistic talking head sequences, there is a potential risk of misuse, such as deepfake creation and manipulation. To address these concerns, we strongly advocate for watermarking or clearly annotating facial sequences generated by our method as synthetic data. Moreover, we will collaborate on deepfake detection research to further ensure that our proposed method is used for positive and constructive applications. We also aim to raise awareness about these risks and encourage collaboration among governments, developers, researchers, and users to jointly prevent the misuse of synthetic video technologies. By fostering collective responsibility and supporting regulatory efforts, we hope to promote the ethical use of AI technologies while mitigating potential harms.

## Acknowledgements

This work was partially supported by JST Moonshot R&D Grant Number JPMJPS2011, CREST Grant Number JPMJCR2015 and Basic Research Grant (Super AI) of Institute for AI and Beyond of the University of Tokyo. In addition, this work was also partially supported by JST SPRING, Grant Number JPMJSP2108.

## References

- Alexanderson, S., Nagy, R., Beskow, J., and Henter, G. E. Listen, denoise, action! audio-driven motion synthesis with diffusion models. *ACM Transactions on Graphics (TOG)*, 42(4):1–20, 2023.
- Aneja, S., Thies, J., Dai, A., and Nießner, M. Facetalk: Audio-driven motion diffusion for neural parametric head models. In *Proc. IEEE Conf. on Computer Vision and Pattern Recognition (CVPR)*, 2024.
- Baevski, A., Zhou, Y., Mohamed, A., and Auli, M. wav2vec 2.0: A framework for self-supervised learning of speech representations. *Advances in neural information processing systems*, 33:12449–12460, 2020.
- Chu, X. and Harada, T. Generalizable and animatable gaussian head avatar. In *The Thirty-eighth Annual Conference on Neural Information Processing Systems*, 2024. URL <https://openreview.net/forum?id=gVM2AZ5xA6>.
- Chu, X., Li, Y., Zeng, A., Yang, T., Lin, L., Liu, Y., and Harada, T. GPAvatar: Generalizable and precise head avatar from image(s). In *The Twelfth International Conference on Learning Representations*, 2024.
- Cudeiro, D., Bolkart, T., Laidlaw, C., Ranjan, A., and Black, M. Capture, learning, and synthesis of 3D speaking styles. In *Proceedings IEEE Conf. on Computer Vision and Pattern Recognition (CVPR)*, pp. 10101–10111, 2019. URL <http://voca.is.tue.mpg.de/>.
- Danecek, R., Black, M. J., and Bolkart, T. EMOCA: Emotion driven monocular face capture and animation. In *Conference on Computer Vision and Pattern Recognition (CVPR)*, pp. 20311–20322, 2022.
- Daněček, R., Chhatre, K., Tripathi, S., Wen, Y., Black, M., and Bolkart, T. Emotional speech-driven animation with content-emotion disentanglement. In *SIGGRAPH Asia 2023 Conference Papers*, pp. 1–13, 2023.
- Défossez, A., Mazaré, L., Orsini, M., Royer, A., Pérez, P., Jégou, H., Grave, E., and Zeghidour, N. Moshi: a speech-text foundation model for real-time dialogue. Technical report, Kyutai, September 2024. URL <http://kyutai.org/Moshi.pdf>.
- Deng, Y., Wang, D., and Wang, B. Portrait4d-v2: Pseudo multi-view data creates better 4d head synthesizer. *arXiv preprint arXiv:2403.13570*, 2024.
- Edwards, P., Landreth, C., Fiume, E., and Singh, K. Jali: an animator-centric viseme model for expressive lip synchronization. *ACM Transactions on graphics (TOG)*, 35(4):1–11, 2016.
- Fan, Y., Lin, Z., Saito, J., Wang, W., and Komura, T. Faceformer: Speech-driven 3d facial animation with transformers. In *Proceedings of the IEEE/CVF Conference on Computer Vision and Pattern Recognition (CVPR)*, 2022.
- Feng, Y., Feng, H., Black, M. J., and Bolkart, T. Learning an animatable detailed 3D face model from in-the-wild images. volume 40, 2021. URL <https://doi.org/10.1145/3450626.3459936>.
- Ho, J., Jain, A., and Abbeel, P. Denoising diffusion probabilistic models. *Advances in neural information processing systems*, 33:6840–6851, 2020.
- Hsu, W.-N., Bolte, B., Tsai, Y.-H. H., Lakhotia, K., Salakhutdinov, R., and Mohamed, A. Hubert: Self-supervised speech representation learning by masked prediction of hidden units. *IEEE/ACM transactions on audio, speech, and language processing*, 29:3451–3460, 2021.
- Huang, X. and Belongie, S. Arbitrary style transfer in real-time with adaptive instance normalization. In *Proceedings of the IEEE international conference on computer vision*, pp. 1501–1510, 2017.
- Li, T., Bolkart, T., Black, M. J., Li, H., and Romero, J. Learning a model of facial shape and expression from 4D scans. *ACM Transactions on Graphics, (Proc. SIGGRAPH Asia)*, 36(6):194:1–194:17, 2017. URL <https://doi.org/10.1145/3130800.3130813>.

- Loshchilov, I. Decoupled weight decay regularization. *arXiv preprint arXiv:1711.05101*, 2017.
- Ma, Z., Zhu, X., Qi, G., Qian, C., Zhang, Z., and Lei, Z. Diff-speaker: Speech-driven 3d facial animation with diffusion transformer. *CoRR*, abs/2402.05712, 2024. URL <https://doi.org/10.48550/arXiv.2402.05712>.
- Nocentini, F., Besnier, T., Ferrari, C., Arguillere, S., Berretti, S., and Daoudi, M. Scantalk: 3d talking heads from unregistered scans. In *Proceedings of the European Conference on Computer Vision (ECCV)*, 2024.
- Paszke, A., Gross, S., Chintala, S., Chanan, G., Yang, E., DeVito, Z., Lin, Z., Desmaison, A., Antiga, L., and Lerer, A. Automatic differentiation in pytorch. 2017.
- Peng, Z., Luo, Y., Shi, Y., Xu, H., Zhu, X., Liu, H., He, J., and Fan, Z. Selftalk: A self-supervised commutative training diagram to comprehend 3d talking faces. In *Proceedings of the 31st ACM International Conference on Multimedia*, pp. 5292–5301, 2023a. doi: 10.1145/3581783.3611734.
- Peng, Z., Wu, H., Song, Z., Xu, H., Zhu, X., He, J., Liu, H., and Fan, Z. Emotalk: Speech-driven emotional disentanglement for 3d face animation. In *Proceedings of the IEEE/CVF International Conference on Computer Vision (ICCV)*, pp. 20687–20697, October 2023b.
- Richard, A., Zollhöfer, M., Wen, Y., De la Torre, F., and Sheikh, Y. Meshtalk: 3d face animation from speech using cross-modality disentanglement. In *Proceedings of the IEEE/CVF International Conference on Computer Vision*, pp. 1173–1182, 2021.
- Sharp, N., Attaiki, S., Crane, K., and Ovsjanikov, M. Diffusionnet: Discretization agnostic learning on surfaces. *ACM Transactions on Graphics (TOG)*, 41(3):1–16, 2022.
- Stan, S., Haque, K. I., and Yumak, Z. Facediffuser: Speech-driven 3d facial animation synthesis using diffusion. In *Proceedings of the 16th ACM SIGGRAPH Conference on Motion, Interaction and Games*, pp. 1–11, 2023. doi: 10.1145/3623264.3624447.
- Sun, Z., Lv, T., Ye, S., Lin, M., Sheng, J., Wen, Y.-H., Yu, M., and Liu, Y.-J. Diffposetalk: Speech-driven stylistic 3d facial animation and head pose generation via diffusion models. *ACM Transactions on Graphics (TOG)*, 43(4), 2024. doi: 10.1145/3658221.
- Sung-Bin, K., Chae-Yeon, L., Son, G., Hyun-Bin, O., Ju, J., Nam, S., and Oh, T.-H. Multitalk: Enhancing 3d talking head generation across languages with multilingual video dataset. In *Interspeech 2024*, pp. 1380–1384, 2024. doi: 10.21437/Interspeech.2024-1794.
- Tan, S., Ji, B., Ding, Y., and Pan, Y. Say anything with any style. In *Proceedings of the AAAI Conference on Artificial Intelligence*, volume 38, pp. 5088–5096, 2024.
- Taylor, S. L., Mahler, M., Theobald, B.-J., and Matthews, I. Dynamic units of visual speech. In *Proceedings of the 11th ACM SIGGRAPH/Eurographics conference on Computer Animation*, pp. 275–284, 2012.
- Tevet, G., Raab, S., Gordon, B., Shafir, Y., Cohen-or, D., and Bermano, A. H. Human motion diffusion model. In *The Eleventh International Conference on Learning Representations*, 2023. URL <https://openreview.net/forum?id=SJ1kSyO2jwu>.
- Tian, K., Jiang, Y., Yuan, Z., PENG, B., and Wang, L. Visual autoregressive modeling: Scalable image generation via next-scale prediction. In *The Thirty-eighth Annual Conference on Neural Information Processing Systems*, 2024. URL <https://openreview.net/forum?id=gojL67CfS8>.
- van den Oord, A., Vinyals, O., and Kavukcuoglu, K. Neural discrete representation learning. In *Proceedings of the 31st International Conference on Neural Information Processing Systems, NIPS’17*, pp. 6309–6318, Red Hook, NY, USA, 2017. Curran Associates Inc. ISBN 9781510860964.
- Wu, S., Li, Y., Yan, Y., Duan, H., Liu, Z., and Zhai, G. Mmhead: Towards fine-grained multi-modal 3d facial animation. In *Proceedings of the 32nd ACM International Conference on Multimedia*, pp. 7966–7975, 2024.
- Xing, J., Xia, M., Zhang, Y., Cun, X., Wang, J., and Wong, T.-T. Codetalker: Speech-driven 3d facial animation with discrete motion prior. In *Proceedings of the IEEE/CVF Conference on Computer Vision and Pattern Recognition*, pp. 12780–12790, 2023.
- Xu, Y., Feng, A. W., Marsella, S., and Shapiro, A. A practical and configurable lip sync method for games. In *Proceedings of Motion on Games*, pp. 131–140. 2013.
- Xu, Y., Chen, B., Li, Z., Zhang, H., Wang, L., Zheng, Z., and Liu, Y. Gaussian head avatar: Ultra high-fidelity head avatar via dynamic gaussians. In *Proceedings of the IEEE/CVF Conference on Computer Vision and Pattern Recognition (CVPR)*, 2024.
- Yang, K. D., Ranjan, A., Chang, J.-H. R., Vemulapalli, R., and Tuzel, O. Probabilistic speech-driven 3d facial motion synthesis: New benchmarks methods and applications. In *Proceedings of the IEEE/CVF Conference on Computer Vision and Pattern Recognition*, pp. 27294–27303, 2024.

- Ye, Z., Zhong, T., Ren, Y., Yang, J., Li, W., Huang, J., Jiang, Z., He, J., Huang, R., Liu, J., et al. Real3d-portrait: One-shot realistic 3d talking portrait synthesis. *arXiv preprint arXiv:2401.08503*, 2024.
- Yi, R., Ye, Z., Sun, Z., Zhang, J., Zhang, G., Wan, P., Bao, H., and Liu, Y.-J. Predicting personalized head movement from short video and speech signal. *IEEE Transactions on Multimedia*, 25:6315–6328, 2022.
- Zhang, H., Liang, Z., Fu, R., Wen, Z., Liu, X., Li, C., Tao, J., and Liang, Y. Letstalk: Latent diffusion transformer for talking video synthesis. *arXiv preprint arXiv:2411.16748*, 2024.
- Zhang, W., Cun, X., Wang, X., Zhang, Y., Shen, X., Guo, Y., Shan, Y., and Wang, F. Sadtalker: Learning realistic 3d motion coefficients for stylized audio-driven single image talking face animation. In *Proceedings of the IEEE/CVF Conference on Computer Vision and Pattern Recognition*, pp. 8652–8661, 2023.
- Zhou, S., Chan, K. C., Li, C., and Loy, C. C. Towards robust blind face restoration with codebook lookup transformer. In *NeurIPS*, 2022.
- Zhu, L., Liu, X., Liu, X., Qian, R., Liu, Z., and Yu, L. Taming diffusion models for audio-driven co-speech gesture generation. In *Proceedings of the IEEE/CVF Conference on Computer Vision and Pattern Recognition*, pp. 10544–10553, 2023.
- Zhuang, Y., Cheng, B., Cheng, Y., Jin, Y., Liu, R., Li, C., Cheng, X., Liao, J., and Lin, J. Learn2talk: 3d talking face learns from 2d talking face. *IEEE Transactions on Visualization and Computer Graphics*, pp. 1–13, 2024. doi: 10.1109/TVCG.2024.3476275.
- Zielonka, W., Bolkart, T., and Thies, J. Towards metrical reconstruction of human faces. In *European Conference on Computer Vision*, pp. 20311–20322, 2022.

## A. Reproducibility

### A.1. More Data Processing Details of VOCASET

For evaluation, we also re-tracked the FLAME (Li et al., 2017) parameters of the VOCASET (Cudeiro et al., 2019) dataset. This is necessary because the original data of VOCASET registers head motion directly onto FLAME meshes rather than FLAME parameters, and also introduces details such as hair that cannot be represented by the FLAME parameters. Since our method and DiffPoseTalk (Sun et al., 2024) works in the FLAME parameter space, we reprocessed VOCASET accordingly. Specifically, we obtained the original VOCASET videos, resampled them to 25 fps, and used EMICA (Feng et al., 2021; Zielonka et al., 2022; Danecek et al., 2022) to extract a 100-dimensional shape vector, a 50-dimensional expression vector, and a 6-dimensional pose vector for evaluation.

For mesh-based baseline methods, we used meshes reconstructed from FLAME parameters instead of the original VOCASET meshes. While this introduces minor differences—such as the absence of hair and subtle expression details—these variations have minimal impact on our primary evaluation, which focuses on lip movements.

### A.2. More Implementation Details

Our model consists of two main components: a multi-scale encoder-decoder and an autoregressive module.

The multi-scale encoder-decoder adopts a transformer-based architecture. Encoder and decoder both consist of 8 layers, each with 8 attention heads and a hidden dimension of 512. The encoder outputs a 64-dimensional codebook representation, while the decoder reconstructs the original expression and pose parameters. During multi-scale quantization, an additional fully connected layer is used in the upsampling process to recover lost information, maintaining an input and output dimension of 64. The codebook consists of 256 vectors, each with a dimensionality of 64.

The autoregressive module is a transformer-based autoregressive model. It has an input and hidden dimension of 768, a conditional vector dimension of 768, and a depth of 12 layers with 12 attention heads. At the input stage, both the codebook features and the audio encoding features are projected to a 768-dimensional space. The audio conditions are incorporated into the transformer layers using adaptive instance normalization (AdaIN) (Huang & Belongie, 2017). After generation through the transformer, a fully connected layer maps the output to a 256-dimensional space, followed by a softmax function to compute the probability distribution over the codebook entries.

We use the AdamW (Loshchilov, 2017) optimizer with an initial learning rate of  $1 \times 10^{-4}$ , trained for 50,000 iterations. A linear decay learning rate scheduler is applied, gradually reducing the learning rate to  $1 \times 10^{-5}$  over the course of training.

### A.3. More Evaluation Details

We generally follow the approach of CodeTalker (Xing et al., 2023) to compute LVE and FFD, and additionally compute the mean mouth opening distance (MMD). Since existing works rarely specify the exact selection of mouth and upper face vertices, we adopt the official FLAME region masks.<sup>1</sup> Specifically, the lip/mouth region consists of 254 vertices from the “lips” area, while the upper face region includes 884 vertices from the “eye\_region” and “forehead” areas.

## B. Preliminaries of 3DMM

We leverage the widely used 3D morphable model (3DMM), FLAME (Li et al., 2017), known for its geometric accuracy and versatility. Due to its realistic rendering capabilities and flexibility, FLAME has been widely adopted in applications such as facial animation, avatar creation, and facial recognition. We use FLAME as our representation for facial motion, construct a multi-scale codebook using FLAME parameters and learn speech-driven autoregression within this codebook, effectively leveraging the priors embedded in FLAME. This approach provides two key advantages: (1) it reduces the high-dimensional complexity of modeling a large number of mesh vertices, and (2) it enables seamless integration with downstream tasks that utilize FLAME-based representations (Chu et al., 2024; Deng et al., 2024; Chu & Harada, 2024; Xu et al., 2024).

The FLAME model represents the head shape as follows:

$$TP(\hat{\beta}, \hat{\theta}, \hat{\psi}) = \bar{T} + BS(\hat{\beta}; S) + BP(\hat{\theta}; P) + BE(\hat{\psi}; E), \quad (8)$$

<sup>1</sup>FLAME\_masks.pkl downloaded from <http://s2017.siggraph.org>.

where  $\bar{T}$  represents the template head avatar mesh,  $BS(\hat{\beta}; S)$  is the shape blend-shape function to account for identity-related shape variation,  $BP(\hat{\theta}; P)$  models jaw and neck pose to correct deformations that cannot be fully explained by linear blend skinning, and the expression blend-shapes  $BE(\hat{\psi}; E)$  capture facial expressions such as eye closure and smiling.

## C. More Discussions on ARTalk

### C.1. The Choice of Audio Encoder

The performance of the audio encoder has a significant impact on the overall model. In this work, we use the HuBERT (Hsu et al., 2021) encoder for experiments. However, HuBERT is primarily designed for longer audio comprehension, which may not be ideal for our windowed input setting. For instance, when the input is as short as 8 frames (320 ms), HuBERT struggles to effectively capture phonetic features.

To address this, we experiment with Mimi (Défossez et al., 2024), an audio encoder better suited for streaming input and short audio segments. As shown in Table 6, Mimi outperforms HuBERT when the input length is short, whereas HuBERT performs better on longer audio segments. We attribute this to Mimi’s design, which prioritizes capturing fine-grained phonetic details in short audio sequences. However, its lower feature dimensionality limits its representational capacity for longer segments compared to HuBERT. Ultimately, the selection of the audio encoder should be guided by the specific requirements of the application, balancing the need for short-term phonetic precision and long-term representational capacity.

Table 6. Different audio encoder performance on TFHP dataset.

METHOD	LVE↓	FFD↓	MOD ↓
MOTION CLIP LENGTH 8 + MIMI	11.01	22.79	2.14
MOTION CLIP LENGTH 8 + HUBERT	11.73	24.89	2.25
MOTION CLIP LENGTH 25 + MIMI	10.33	19.65	1.99
MOTION CLIP LENGTH 25 + HUBERT	10.20	19.00	1.97
MOTION CLIP LENGTH 50 + MIMI	10.10	19.16	1.95
MOTION CLIP LENGTH 50 + HUBERT	9.78	18.03	1.89
MOTION CLIP LENGTH 100 + MIMI	9.97	18.48	1.93
MOTION CLIP LENGTH 100 + HUBERT	<b>9.34</b>	<b>18.15</b>	<b>1.81</b>

### C.2. Performance of Multi-scale VQ Autoencoder

The overall performance of the model is inherently influenced by the VQ autoencoder, which serves as the upper bound for the final model’s performance. Here in Table 7, we present the performance of VQ autoencoder trained with different clip lengths. We did not observe a significant impact of clip length on the performance of the VQ autoencoder. For the autoregressive generation results under different segment length settings, please refer to the Table 5 in the main paper.

Table 7. VQ Autoencoder performance on TFHP dataset.

METHOD	LVE↓	FFD↓	MOD ↓
MOTION CLIP LENGTH 8	1.96	8.81	0.43
MOTION CLIP LENGTH 25	1.97	9.57	0.44
MOTION CLIP LENGTH 50	2.19	9.54	0.47
MOTION CLIP LENGTH 100	2.08	8.97	0.45

## D. User Study Details

We collected a total of 28 survey responses, with each participant answering 84 questions (corresponding to 84 pairwise comparison trials), for a total of 2352 comparisons. Among these, 63 comparisons were conducted on the TFHP dataset and 21 on the VOCASET dataset. To mitigate potential biases caused by random or preferential selections, we randomized the display order of our method and the baseline in each trial. Which means in each comparison, one of the videos (A or B) was generated by our method, but the assignment was randomized.

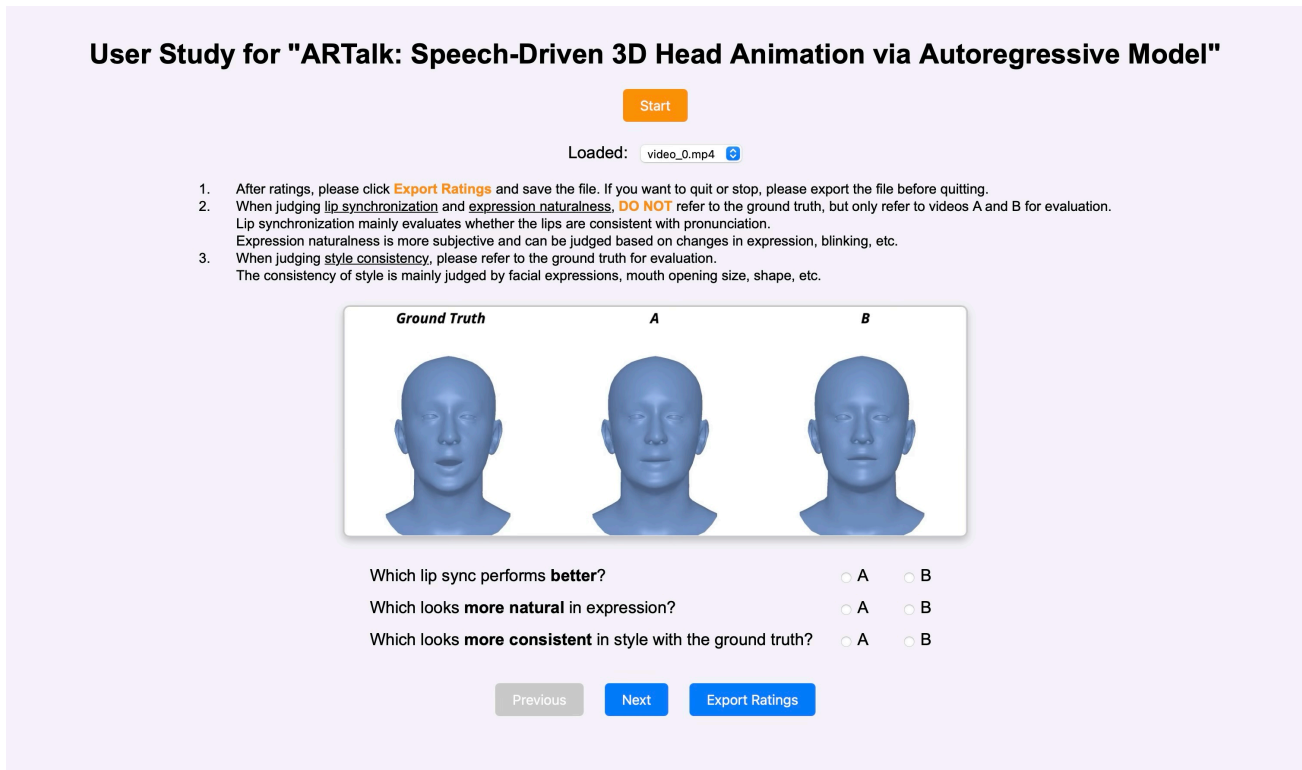


Figure 6. The interface of our user study. Users evaluate each video based on three criteria: lip synchronization, expression naturalness, and style consistency. The first two are judged by comparing method A and B, while style consistency is assessed with reference to the ground truth. One of the videos (A or B) is generated by our method, and the other by a baseline method, with their order randomized.

For each comparison, users were asked three questions. The first two questions follow prior studies (Fan et al., 2022; Xing et al., 2023), assessing the quality of lip synchronization and the perceived naturalness of expressions. Additionally, we introduce a third question to evaluate the consistency of the generated animation with the ground truth style. The questions presented to users were as follows: Which lip sync performs better? Which looks more natural in expression? Which looks more consistent in style with the ground truth? All three questions are single-choice, requiring users to select either A or B.



Figure 7. We reconstruct the avatar using GAGAvatar (Chu & Harada, 2024) and drive it with our ARTalk model, enabling speech-driven dynamic avatar generation.

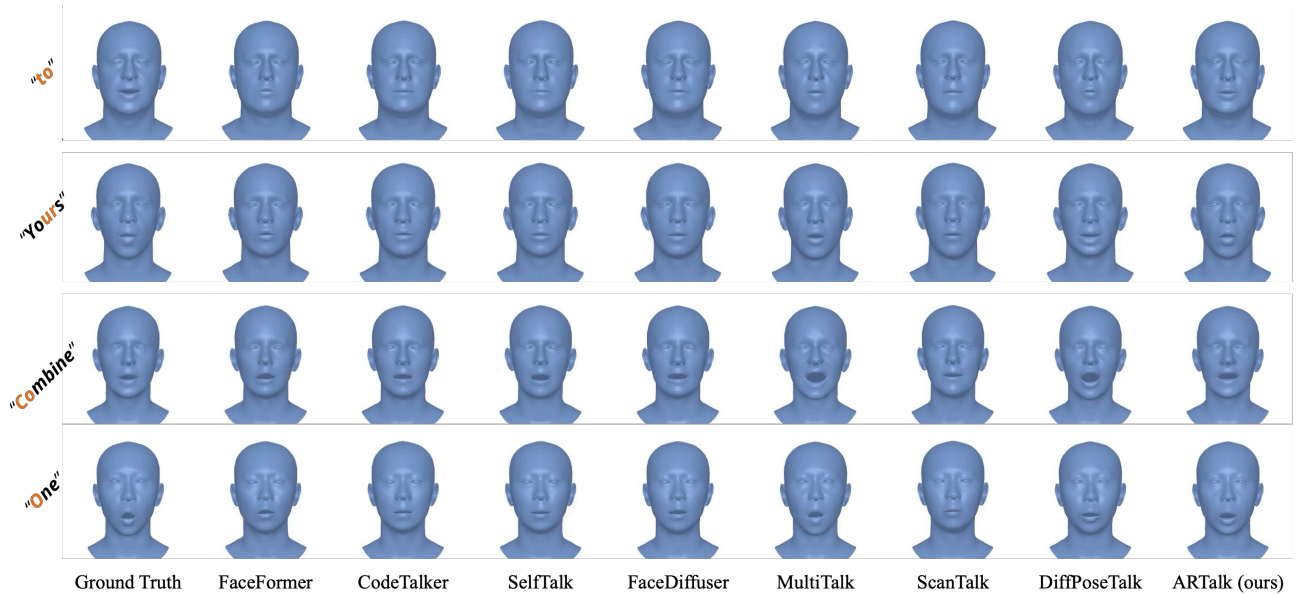


Figure 8. The interface of our user study.

## E. Integration with Downstream Tasks

Our method can be integrated into various FLAME-based downstream applications, enabling a wider range of use cases. While this extends beyond the primary scope of this paper, we also demonstrate its application in GAGAvatar (Chu & Harada, 2024). As shown in Figure 7, our method can generate control signals for GAGAvatar, effectively transforming it into a speech-driven one-shot dynamic avatar reconstruction method.

## F. More Qualitative Results

We present additional qualitative comparison results in Figure 8. However, we strongly recommend referring to the supplementary video for a more comprehensive comparison of different methods.